Title
Pelagic Methane Sink Enhanced by Benthic Methanotrophs Ejected From a Gas Seep

Journal
Geophysical Research Letters, 48(20)

ISSN
0094-8276

Authors
Jordan, SFA
Gräwe, U
Treude, T
et al.

Publication Date
2021-10-28

DOI
10.1029/2021gl094819

Peer reviewed

Geophysical Research Letters

RESEARCH LETTER
10.1029/2021GL094819

Pelagic Methane Sink Enhanced by Benthic Methanotrophs Ejected From a Gas Seep

S. F. A. Jordan[1], U. Gräwe[1], T. Treude[2,3], E. M. van der Lee[4], J. Schneider von Deimling[5], G. Rehder[1], and O. Schmale[1]

[1]Leibniz Institute for Baltic Sea Research Warnemünde, Rostock, Germany, [2]Department of Earth, Planetary, and Space Sciences, University of California Los Angeles, Los Angeles, CA, USA, [3]Department of Atmospheric and Oceanic Sciences, University of California Los Angeles, Los Angeles, CA, USA, [4]German Federal Maritime and Hydrographic Agency, Rostock, Germany, [5]Christian-Albrechts-Universität zu Kiel, Institute for Geosciences, Marine Geophysics & Hydroacoustics, Kiel, Germany

Key Points:

- The ejection of benthic methanotrophs from the gas seep site can explain the methanotroph's abundance in the down-current methane plume
- The seep-induced inoculation of the water column with methanotrophs decreased the pelagic methane turnover time by a factor of about five
- Our particle-tracking model showed that tides controlled the areal distribution of methane and methanotrophs released by the seep site

Supporting Information:

Supporting Information may be found in the online version of this article.

Correspondence to:

S. F. A. Jordan and O. Schmale, Sebastian.Jordan@io-warnemuende.de; Oliver.Schmale@io-warnemuende.de

Citation:

Jordan, S. F. A., Gräwe, U., Treude, T., van der Lee, E. M., Schneider von Deimling, J., Rehder, G., & Schmale, O. (2021). Pelagic methane sink enhanced by benthic methanotrophs ejected from a gas seep. *Geophysical Research Letters*, *48*, e2021GL094819. https://doi.org/10.1029/2021GL094819

Received 18 JUN 2021
Accepted 1 OCT 2021

Author Contributions:

Conceptualization: O. Schmale
Formal analysis: S. F. A. Jordan, U. Gräwe, T. Treude, E. M. van der Lee, J. Schneider von Deimling
Funding acquisition: T. Treude, O. Schmale
Investigation: S. F. A. Jordan, T. Treude, J. Schneider von Deimling, O. Schmale

Abstract Cold seeps represent hot spots of seabed-derived methane emissions to the water column, where physical and biological barriers regulate transport of methane to the atmosphere. In our study, we used a methane point source in the North Sea to investigate water-column methane dynamics within the dispersing plumes. The study is based on methane concentration, distribution and activity of methane-oxidizing bacteria (MOB), and oceanographic observations. Our findings suggest the ejection of benthic MOB into the water column by sediment resuspension and gas-bubble-mediated transport. An applied particle-tracking model demonstrated that the ejection of $4.29 \pm 1.9 \times 10^{12}$ MOB cells s^{-1} from the seep site would produce the MOB abundance detected in the down-current water body. The benthic MOB inoculant accelerated methane oxidation rates by a factor of five. Our study highlights the importance of the bentho-pelagic transport of microorganisms at seep sites and their feedback on the pelagic methane sink.

Plain Language Summary In the marine system, the greenhouse gas methane is primarily produced in sediments. Under specific geologic conditions, methane can accumulate in the sediment and be released as gas bubbles. Such gas seepage also occurs at abandoned oil or gas-drilling sites. However, direct transport of methane from submarine seeps to the atmosphere is only likely in shallow regions, as ascending bubbles release most of their methane quickly into the surrounding water. Methanotrophic bacteria living in the top sediment layer and the water column metabolize the dissolved methane. These methanotrophs can be transported from the sediment into the water column by gas bubbles or sediment resuspension. To understand the effect of the transported methanotrophs on the methane removal in the water column, we focused on an abandoned oil-drilling site in the North Sea that has been emitting methane gas bubbles since 1990. We took water samples from different depths near the drilling site and this showed that the transported methanotrophs accelerated methane oxidation rates by a factor of about five. Additionally, we used a numerical model to estimate the number of methanotrophs ejected from the seep site and traced their distribution in the dispersing plume.

1. Introduction

Sediments along continental margins harbor vast amounts of methane, a potent greenhouse gas whose atmospheric concentration has almost constantly been increasing since pre-industrial times (Saunois et al., 2016). Seabed-derived methane transport to the sea surface is hampered by physical (water column density stratification; Schmale et al., 2016) and biological (anaerobic and aerobic methane oxidation; Whiticar, 2020) barriers. The dominant pathway of pelagic microbial methane oxidation follows the reaction (Equation 1):

$$CH_4 + 2O_2 \rightarrow CO_2 + 2H_2O \quad (1)$$

and is mediated by methanotrophic bacteria (MOB), which represent the final sink of methane before its escape into the atmosphere. Transportation of sedimentary methane to the sea surface is facilitated via two different pathways: (a) advective and diffusive fluxes of dissolved methane that reach the surface water over relatively long time scales (Matveeva et al., 2015) and (b) gas bubble ebullition that allows a more rapid

Methodology: S. F. A. Jordan, U. Gräwe, T. Treude
Project Administration: O. Schmale
Resources: J. Schneider von Deimling, O. Schmale
Software: U. Gräwe
Supervision: O. Schmale
Visualization: S. F. A. Jordan, U. Gräwe, E. M. van der Lee, J. Schneider von Deimling
Writing – original draft: S. F. A. Jordan
Writing – review & editing: U. Gräwe, T. Treude, E. M. van der Lee, J. Schneider von Deimling, G. Rehder, O. Schmale

and efficient methane transport (Leifer & Patro, 2002). While the dissolved methane fraction is accessible to methanotrophs, the gaseous fraction can bypass pelagic methane oxidation (Knittel & Boetius, 2009). However, direct transport of methane into the atmosphere by gas bubbles is likely only in shallow seep regions, because after their liberation from the seafloor, the ascending bubbles release most of their methane (75%–100%) within the first 100 m (McGinnis et al., 2006). Continuous transfer of methane from rising bubbles into the water creates methane-laden water masses, which are transported away from the methane source by currents (Kessler et al., 2011; Steinle et al., 2015). Entrainment of benthic MOB into plume waters via resuspension of sediment (Steinle et al., 2016) and/or bubble-mediated dislocation (Jordan et al., 2020; Schmale et al., 2015; Schubert et al., 2006) can support pelagic methane turnover. In bubble-mediated dislocation processes, particles and microorganisms adsorb to the gas/water bubble interface (Wan & Wilson, 1994) during the buoyancy-driven passage of bubbles through the sediment. After being emitted into the water column, these surfactants are released from the bubble due to shear stress and bubble dissolution (Blanchard, 1975; Leifer & Patro, 2002). However, detailed knowledge of bentho-pelagic MOB transport controls and their effect on the pelagic methane turnover remains vague, but is a prerequisite for a proper understanding of the fate of methane in the water column.

To characterize the ejection of benthic MOB from a seep into the water column and quantify its impact on pelagic methane turnover, we selected an isolated seep site to ensure that related plume waters are not affected by adjacent seep locations. The study was conducted in summer 2016 at the abandoned well site 22/4b (hereafter 'Blowout', water depth ~100 m) in the North Sea during the RV Poseidon expedition POS 504 (Figure 1a). At this site, a drilling operation in 1990 caused a massive gas release into the water column (Rehder et al., 1998), resulting in the formation of a crater with a diameter of ~60 m and a depth of ~20 m from which gas is still being released into the water column (Schneider von Deimling et al., 2015). We studied methane dynamics as well as activity and size of the pelagic methanotrophic community through quantification of methane concentrations, methane oxidation rates (MOx) and MOB abundances. Studies were supplemented by oceanographic investigations to describe the current regime and water mass movement using an acoustic Doppler current profiler deployed near the Blowout crater. Two water-column transects positioned orthogonal to the residual background current were set up: one up-current of the Blowout (hereafter 'IN' transect) and one down-current (hereafter 'OUT' transect; Figure 1, Figures S1 and S2 in Supporting Information S1). To obtain a robust estimate of the bentho-pelagic MOB transport from the Blowout site and its impact on the methane turnover within the dispersing plume, we studied the characteristics of plume-affected and plume-unaffected waters. The dispersion of the MOB after their ejection from the Blowout into the water column was investigated using a Lagrangian particle-tracking model (Bauer et al., 2013, 2014) forced by the output of a numerical ocean model (Klingbeil & Burchard, 2013).

2. Results and Discussion

As the waters in the Blowout area are seasonally stratified from April/May until October/November (Nauw, de Haas, et al., 2015), deep-water masses are largely decoupled from the mixed layer during this period. Hydroacoustic images of the water column showed that the Blowout crater's gas-bubble release created an extensive bubble plume divided into two parts: one part stayed below the lower thermocline (located at 35 m water depth), and the other part was breaking through the less pronounced upper thermocline (located at ~20 m; Figure 1b and Figure S3 in Supporting Information S1). Previous studies showed that gas bubbles released from the Blowout crater partly dissolve during their passage through the water column and thereby create a plume of dissolved methane (Leifer et al., 2015; Schneider von Deimling et al., 2015). In our study, the plume was mapped inside the sub-thermocline water body within a distance of 1.6 km from the Blowout (Figure 2, Table S1). A comparison of the sub-thermocline methane inventories along the two transects showed a nearly two-fold higher inventory in the OUT compared to the IN transect (Figure 3a and Table 1). Moreover, only ~9% (IN) and ~23% (OUT) of the total methane inventory was located in the upper 35 m of the water column, indicating a quick release of methane from the bubbles during their ascent through the sub-thermocline water column (Leifer et al., 2015) and a hampered transport of dissolved methane through the lower thermocline (Nauw, Linke, et al., 2015).

Similar to the methane distribution, the highest MOx capacity was detected in the OUT transect below the lower thermocline (~94% of the total MOx capacity; Table 1), consistent with the northward residual

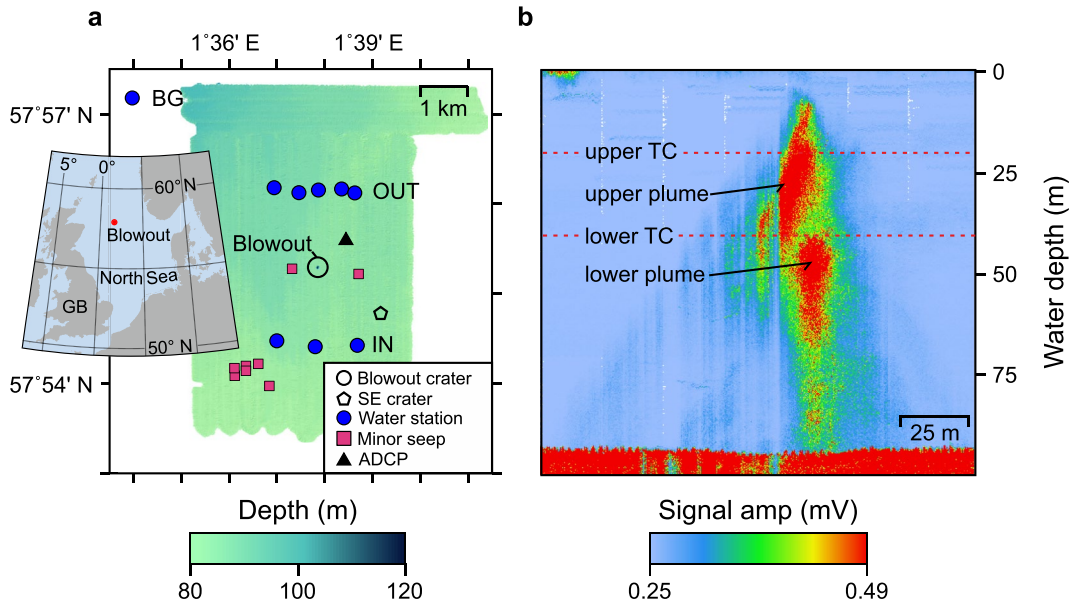

Figure 1. Study site and gas bubble flare image above the Blowout. (a), Mercator map showing the bathymetry around the Blowout crater (green-blue background). The inset displays an overview of the North Sea and the position of the Blowout (red circle). The station map shows the positions sampled (blue circles) for the IN and OUT transects, the background station (BG), and the station directly above the Blowout crater (encircled). Natural seeps (red squares) and a smaller south-eastern crater (pentagon) are also shown. The acoustic Doppler current profiler (ADCP, black triangle) is northwest of the Blowout. Positions and sampling dates are listed in Table S4. (b), Echogram multibeam view of the Blowout (full width: 155 m). Signal amplitudes (Signal amp) are mapped with a linear color bar. A lower plume is visible until ~35 m water depth while an upper plume reaches the sea surface. The red dotted line represents the upper and lower thermocline at ~20 and ~35 m, respectively. The cruising speed during hydroacoustic data recording was ~0.5 kn.

transport. A comparison of the sub-thermocline MOB inventories along the IN and OUT transects showed a 1.3-fold higher inventory in the down-current positioned OUT transect (Figure 3b), indicating an immediate impact of the methane point source on the pelagic MOB abundance. Compared with the background station 5 km away from the Blowout, the MOB cell concentrations in the two transects were up to 10-fold higher than at the background station (Figure S4 in Supporting Information S1). The substantial enrichment of MOB cells in the near field of the Blowout was reproduced by our particle-tracking model (Figure 4). The model demonstrated that the northward-oriented spreading of the MOB cell plume was affected by tidal cycles, which caused a clockwise oscillating motion of the plume (Movie S1). This movement forced the plume multiple times into the vicinity of the Blowout, resulting in repeated collections of MOB cells ejected from the seep site. We disregarded MOB community growth effects on the plume MOB stock, because the water and associated MOB community are swept away from the Blowout regions on times scales shorter than average MOB cell doubling times (~3 days; Kessler et al., 2011; Movie S1 and Figure S5 in Supporting Information S1).

Patches of elevated MOB cell concentrations were detected in the surface waters at station O3 and O5 of the OUT transect (Figure 2c), presumably indicating a bubble-mediated (Jordan et al., 2020; Schmale et al., 2015) cross-thermocline transport of these cells. Particles (including bacteria) attached to bubble surfaces can thus be transported across strong density gradients, such as thermoclines, that inhibit an exchange of particles or dissolved substances by pure diffusion or advection (Nauw, Linke, et al., 2015; Schmale et al., 2016). Leifer et al. (2015) proposed that the bubble rise velocity is accelerated by the bubble-plume-induced upwelling flow (Schneider von Deimling et al., 2015), which in turn favors the survival of the bubbles and therewith bubble-mediated transportation of MOB cells into the mixed layer.

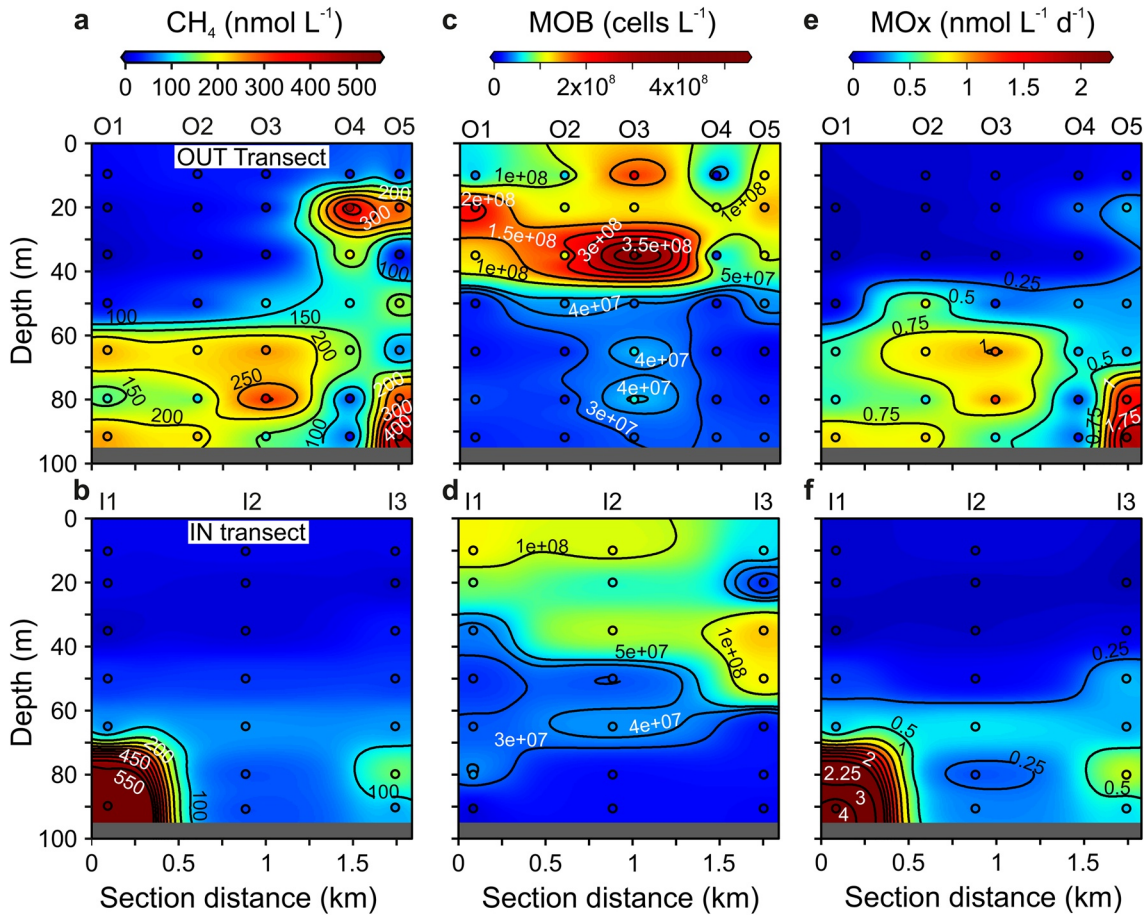

Figure 2. Sections of methane-related biogeochemical parameters along the IN and OUT transects. (a), (c), (e), The sections of the OUT transect with five stations (west to east O1–O5) and (b), (d), (f), the IN transect with three stations (west to east I1–I3) are depicted. (a + b), The water-column methane concentration, (c + d), abundance of aerobic methane-oxidizing bacteria (MOB), and (e + f), methane oxidation rates (MOx) are shown. The parameters are displayed over depth and along the transect distance. The gray area at the bottom of each graph indicates the seafloor.

Our Lagrangian particle-tracking model (Figure 4) indicated that 4.29 ± 1.9 × 10^{12} MOB cells s^{-1} were released from the Blowout into the water column to maintain the sub-thermocline MOB cell inventories measured along the IN and OUT transects (Figure 3b). Based on a gas release of 90 L s^{-1} from the crater (Leifer, 2015), we computed a MOB cell-ejection rate of 4.8 × 10^{10} MOB cells L^{-1} gas. A comparison of the bubble-mediated MOB cell transport in the Coal Oil Point seep field at the Isla Vista super seep (1.2 × 10^{11} MOB cells m^{-2} d^{-1}, 700 vents m^{-2}; Jordan et al., 2020) with results of our study (1.35 ± 0.6 × 10^{15} MOB cells m^{-2} d^{-1}, based on a seepage area within the crater of ~275.5 m^2; Leifer, 2015), suggests that MOB cell transport per square meter of active seepage area was four orders of magnitude higher at the Blowout. Based on this comparison, we propose that the resuspension of crater sediment (Schneider von Deimling et al., 2015) played an essential role for the coupling of benthic and pelagic MOB communities at the Blowout, in addition to the bubble-mediated transport of MOB cells, which was the dominant transport process identified in the Coal Oil Point seep field (Jordan et al., 2020). This conclusion is further supported by phylogenetic analysis indicating similarities in the microbial community composition between Blowout crater surface sediments and bottom water (Steinle et al., 2016), as well as an elevated turbidity in the crater interior (Movies S2 and S3, Figure S8 in Supporting Information S1). Other studies showed that the bubbles emitted from the crater accelerate an upwelling flow that supports the upward transportation of resuspended sediment particles and their enrichment below the lower thermocline (Schneider von Deimling et al., 2015; Wilson et al., 2015).

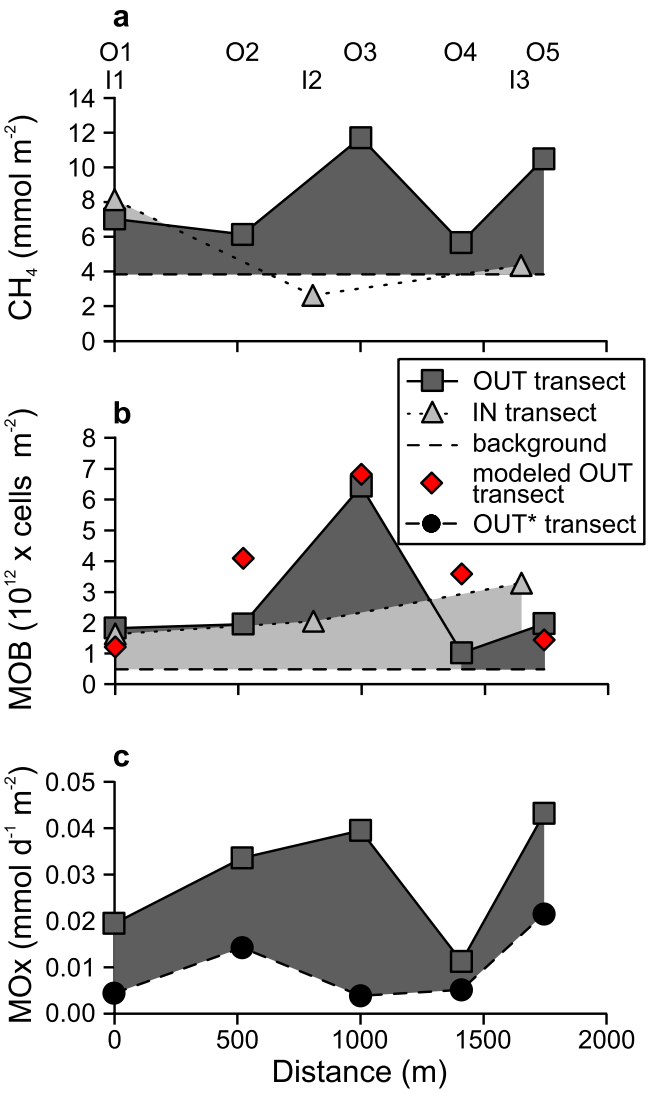

Figure 3. Depth-integrated inventories along the IN and OUT transects. (a), Methane, (b), methane-oxidizing bacteria (MOB) for the IN (light gray triangles) and OUT (dark gray squares) transects and for the modeled OUT transect (red diamonds) were integrated over the respective transect grid and for the sub-thermocline waters (35–90 m). The dashed line (in a + b) indicates the values measured at the background station. In (c), methane oxidation rates (MOx) are shown for the OUT (gray squares) and OUT* (black circles) transects. The latter was calculated as the MOB cell abundances of the background site multiplied by the cell-specific methane oxidation rates of the OUT transect.

The MOB cell-enrichment detected in the center of the OUT transect (Figure 2c, station O3, 5.3×10^8 MOB cells L^{-1} at 35 m depth) likely resulted from such a transport mechanism.

Our model results suggest that the MOB enrichment in the plume waters (Figure 4 and Figure S6 in Supporting Information S1) results from the ejection of cells from Blowout crater sediments into the water column. Following this assumption, we used data obtained from the OUT transect (Table S1) to estimate the impact on the efficacy of the pelagic methane sink. We deduced a methane oxidation capacity for the OUT transect unaffected by the ejection of MOB cells (hereafter OUT*), by multiplying the cell-specific methane oxidation rate at each depth as measured along the OUT transect by the MOB cell count determined at the corresponding depth at the background station (Table S2). This approach results in an upper estimate of the methane oxidation capacity within the OUT* transect, since the particle-tracking model indicates that the background station was still slightly impacted by the Blowout MOB ejection (Movie S1). The comparison of the methane oxidation inventories (Figure 3c and Table S3) of the OUT and OUT* transects suggests that the methane oxidation capacity along the OUT transect (~0.076 mol m^{-1} d^{-1}) was ~4.6 times higher compared to the OUT* transect (~0.017 mol m^{-1} d^{-1}). The elevated methane oxidation capacity along the OUT transect led to a reduction of the methane turnover time by the same factor (turnover time along OUT* of 883 vs. 183 days for the OUT transect, Table 1), suggesting that the ejection of MOB cells considerably increased the efficacy of the pelagic methane sink.

3. Conclusions

Pelagic methane oxidation is the final sink for seabed-derived methane before its release into the atmosphere. Especially at cold vents, where large amounts of methane bypass the sedimentary microbial methane sinks, the role of pelagic methane oxidation in reducing the methane emission from the ocean becomes even more important. Pelagic methane turnover at highly active seeps is controlled by environmental factors such as methane availability (Crespo-Medina et al., 2014), differential circulation patterns (Steinle et al., 2015), and redox conditions (Kessler et al., 2011). Our new results demonstrate that, apart from these factors, the dislocation of benthic methanotrophs into the water column can spontaneously boost the methane oxidation capacity within the dispersing methane plume. This transport mechanism becomes even more critical at seep sites characterized by water residence times that are too short to allow the relatively slow-growing methanotrophic community to establish a resilient methane sink. However, for a comprehensive understanding of methane dynamics in a dispersing plume we propose further studies to investigate the survival, potential growth and activity change of benthic MOB in the aging plume waters and trace shifts in the microbial community composition. Even though the impact of environmental factors on MOB abundance and activity may vary between seep locations, we contend that the bentho-pelagic transportation of methanotrophs creates a positive feedback on the pelagic methane sink through the reduction of methane turnover time and atmospheric flux.

Table 1
Methane-Related Biogeochemical Parameters Across the IN and OUT Transects

Upper water column (0–35 m)	IN	OUT	OUT*
MOB inventory	5.47×10^{15} cells m^{-1}	7.88×10^{15} cells m^{-1}	
CH_4 inventory	0.7 mol m^{-1}	4.2 mol m^{-1}	
MOx capacity	0.0013 mol m^{-1} d^{-1}	0.0052 mol m^{-1} d^{-1}	
Sub-thermocline water body (35–90 m)	**IN**	**OUT**	**OUT***
MOB inventory	3.74×10^{15} cells m^{-1}	5.01×10^{15} cells m^{-1}	8.61×10^{14} cells m^{-1}
CH_4 inventory	7.3 mol m^{-1}	14.0 mol m^{-1}	14.0 mol m^{-1}
MOx capacity	0.031 mol m^{-1} d^{-1}	0.076 mol m^{-1} d^{-1}	0.017 mol m^{-1} d^{-1}
k'	0.0043 d^{-1}	0.0055 d^{-1}	0.0012 d^{-1}
CH_4 turnover time	233 d	183 d	833 d

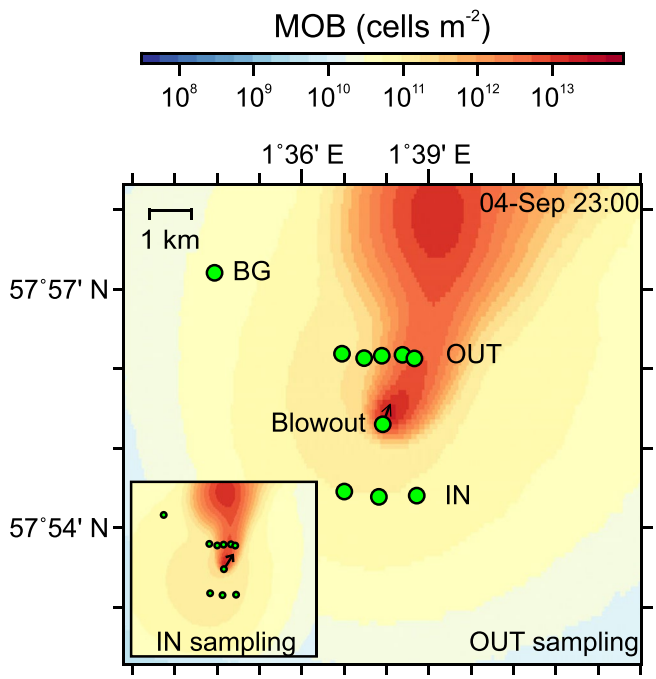

Figure 4. Snapshots of the modeled methane-oxidizing bacteria (MOB) spatial distributions. Modeled spatial distributions of MOB on the indicated sampling dates for the OUT transect and the IN transect (inset, September 5, 23:00 UTC) over a depth range of 35–90 m. The color-coding indicates the MOB cell concentration integrated over the respective depth range. Green dots represent the transects' sampling stations (OUT, IN), and the background station (BG). The arrow at the Blowout position indicates the instantaneous current direction. Movie S1 shows the spatial and temporal MOB distribution. To ensure a comparable orientation of the MOB plume between the two transects' samplings, the water column studies were conducted at similar tidal situation (temporal offset of ~24 h).

Conflict of Interest

The authors declare no conflicts of interest relevant to this study.

Data Availability Statement

Derived data and the data output from the Lagrangian particle tracking model supporting the findings of this study are available at https://doi.io-warnemuende.de/10.12754/data-2021-0003.

Acknowledgments
We thank the captain and crew of R/V Poseidon (POS504) for the friendly and professional support at sea. We greatly acknowledge the ROV-team (GEOMAR) for operating the ROV PHOCA during the expedition. We further thank Stefan Krause (GEOMAR) for help with the CARD-FISH method setup. The work was funded by the Deutsche Forschungsgemeinschaft (DFG), German Research Foundation–SCHM 2530/71 and SCHU 1416/1-4.

References

Bauer, R. K., Gräwe, U., Stepputtis, D., Zimmermann, C., & Hammer, C. (2014). Identifying the location and importance of spawning sites of Western Baltic herring using a particle backtracking model. *ICES Journal of Marine Science*, *71*(3), 499–509. https://doi.org/10.1093/icesjms/fst163

Bauer, R. K., Stepputtis, D., Gräwe, U., Zimmermann, C., & Hammer, C. (2013). Wind-induced variability in coastal larval retention areas: A case study on Western Baltic spring-spawning herring. *Fisheries Oceanography*, *22*(5), 388–399. https://doi.org/10.1111/fog.12029

Blanchard, D. C. (1975). Bubble scavenging and the water-to-air transfer of organic material in the sea. In *Applied chemistry at protein interfaces* (pp. 360–387). https://doi.org/10.1021/ba-1975-0145.ch018

Crespo-Medina, M., Meile, C. D., Hunter, K. S., Diercks, A.-R., Asper, V. L., Orphan, V. J., et al. (2014). The rise and fall of methanotrophy following a deepwater oil-well blowout. *Nature Geoscience*, *7*(6), 423–427. https://doi.org/10.1038/ngeo2156

Jordan, S. F. A., Treude, T., Leifer, I., Janßen, R., Werner, J., Schulz-Vogt, H., & Schmale, O. (2020). Bubble-mediated transport of benthic microorganisms into the water column: Identification of methanotrophs and implication of seepage intensity on transport efficiency. *Scientific Reports*, *10*(1), 4682. https://doi.org/10.1038/s41598-020-61446-9

Kessler, J. D., Valentine, D. L., Redmond, M. C., Du, M., Chan, E. W., Mendes, S. D., et al. (2011). A persistent oxygen anomaly reveals the fate of spilled methane in the deep Gulf of Mexico. *Science*, *331*(6015), 312–315. https://doi.org/10.1126/science.1199697

Klingbeil, K., & Burchard, H. (2013). Implementation of a direct nonhydrostatic pressure gradient discretisation into a layered ocean model. *Ocean Modelling*, *65*, 64–77. https://doi.org/10.1016/j.ocemod.2013.02.002

Knittel, K., & Boetius, A. (2009). Anaerobic oxidation of methane: Progress with an unknown process. *Annual Review of Microbiology*, *63*(1), 311–334. https://doi.org/10.1146/annurev.micro.61.080706.093130

Leifer, I. (2015). Seabed bubble flux estimation by calibrated video survey for a large blowout seep in the North Sea. *Marine and Petroleum Geology*, *68*, 743–752. https://doi.org/10.1016/j.marpetgeo.2015.08.032

Leifer, I., & Patro, R. K. (2002). The bubble mechanism for methane transport from the shallow sea bed to the surface: A review and sensitivity study. *Continental Shelf Research*, *22*(16), 2409–2428. https://doi.org/10.1016/S0278-4343(02)00065-1

Leifer, I., Solomon, E., Schneider von Deimling, J., Rehder, G., Coffin, R., & Linke, P. (2015). The fate of bubbles in a large, intense bubble megaplume for stratified and unstratified water: Numerical simulations of 22/4b expedition field data. *Marine and Petroleum Geology*, *68*, 806–823. https://doi.org/10.1016/j.marpetgeo.2015.07.025

Matveeva, T., Savvichev, A. S., Semenova, A., Logvina, E., Kolesnik, A. N., & Bosin, A. A. (2015). Source, origin, and spatial distribution of shallow sediment methane in the Chukchi Sea. *Oceanography*, *28*(3), 202–217. https://doi.org/10.5670/oceanog.2015.66

McGinnis, D. F., Greinert, J., Artemov, Y., Beaubien, S. E., & Wüest, A. (2006). Fate of rising methane bubbles in stratified waters: How much methane reaches the atmosphere? *Journal of Geophysical Research*, *111*, C09007. https://doi.org/10.1029/2005JC003183

Nauw, J., de Haas, H., & Rehder, G. (2015). A review of oceanographic and meteorological controls on the North Sea circulation and hydrodynamics with a view to the fate of North Sea methane from well site 22/4b and other seabed sources. *Marine and Petroleum Geology*, *68*, 861–882. https://doi.org/10.1016/j.marpetgeo.2015.08.007

Nauw, J., Linke, P., & Leifer, I. (2015). Bubble momentum plume as a possible mechanism for an early breakdown of the seasonal stratification in the northern North Sea. *Marine and Petroleum Geology*, *68*, 789–805. https://doi.org/10.1016/j.marpetgeo.2015.05.003

Rehder, G., Keir, R. S., Suess, E., & Pohlmann, T. (1998). The multiple sources and patterns of methane in North Sea waters. *Aquatic Geochemistry*, *4*(3–4), 403–427. https://doi.org/10.1023/A:1009644600833

Saunois, M., Bousquet, P., Poulter, B., Peregon, A., Ciais, P., Canadell, J. G., et al. (2016). The global methane budget 2000–2012. *Earth System Science Data*, *8*(2), 697–751. https://doi.org/10.5194/essd-8-697-2016

Schmale, O., Krause, S., Holtermann, P., Power Guerra, N. C., & Umlauf, L. (2016). Dense bottom gravity currents and their impact on pelagic methanotrophy at oxic/anoxic transition zones. *Geophysical Research Letters*, *43*(10), 5225–5232. https://doi.org/10.1002/2016GL069032

Schmale, O., Leifer, I., Deimling, J. S., Von Stolle, C., Krause, S., Kießlich, K., et al. (2015). Bubble Transport Mechanism: Indications for a gas bubble-mediated inoculation of benthic methanotrophs into the water column. *Continental Shelf Research*, *103*, 70–78. https://doi.org/10.1016/j.csr.2015.04.022

Schneider von Deimling, J., Linke, P., Schmidt, M., & Rehder, G. (2015). Ongoing methane discharge at well site 22/4b (North Sea) and discovery of a spiral vortex bubble plume motion. *Marine and Petroleum Geology*, *68*, 718–730. https://doi.org/10.1016/j.marpetgeo.2015.07.026

Schubert, C. J., Durisch-Kaiser, E., Holzner, C. P., Klauser, L., Wehrli, B., Schmale, O., et al. (2006). Methanotrophic microbial communities associated with bubble plumes above gas seeps in the Black Sea. *Geochemistry, Geophysics, Geosystems*, *7*(4), Q04002. https://doi.org/10.1029/2005GC001049

Steinle, L., Graves, C. A., Treude, T., Ferré, B., Biastoch, A., Bussmann, I., et al. (2015). Water column methanotrophy controlled by a rapid oceanographic switch. *Nature Geoscience*, *8*(5), 378–382. https://doi.org/10.1038/ngeo2420

Steinle, L., Schmidt, M., Bryant, L., Haeckel, M., Linke, P., Sommer, S., et al. (2016). Linked sediment and water-column methanotrophy at a man-made gas blowout in the North Sea: Implications for methane budgeting in seasonally stratified shallow seas. *Limnology & Oceanography*, *61*(S1), S367–S386. https://doi.org/10.1002/lno.10388

Wan, J., & Wilson, J. L. (1994). Visualization of the role of the gas-water interface on the fate and transport of colloids in porous media. *Water Resources Research*, *30*(1), 11–23. https://doi.org/10.1029/93WR02403

Whiticar, M. J. (2020). The biogeochemical methane cycle. In H. Wilkes (Ed.), *Hydrocarbons, oils and lipids: Diversity, origin, chemistry and fate* (pp. 1–78). Springer. https://doi.org/10.1007/978-3-319-54529-5_5-1

Wilson, D. S., Leifer, I., & Maillard, E. (2015). Megaplume bubble process visualization by 3D multibeam sonar mapping. *Marine and Petroleum Geology*, *68*, 753–765. https://doi.org/10.1016/j.marpetgeo.2015.07.007

References From the Supporting Information

Bussmann, I., Matousu, A., Osudar, R., & Mau, S. (2015). Assessment of the radio ^{3}H-CH_4 tracer technique to measure aerobic methane oxidation in the water column. *Limnology and Oceanography: Methods*, *13*(6), 312–327. https://doi.org/10.1002/lom3.10027

Eller, G., Stubner, S., & Frenzel, P. (2001). Group-specific 16S rRNA targeted probes for the detection of type I and type II methanotrophs by fluorescence in situ hybridisation. *FEMS Microbiology Letters*, *198*(2), 91–97. https://doi.org/10.1111/j.1574-6968.2001.tb10624.x

Gräwe, U., Holtermann, P., Klingbeil, K., & Burchard, H. (2015). Advantages of vertically adaptive coordinates in numerical models of stratified shelf seas. *Ocean Modelling*, *92*, 56–68. https://doi.org/10.1016/j.ocemod.2015.05.008

Jakobs, G., Holtermann, P., Berndmeyer, C., Rehder, G., Blumenberg, M., Jost, G., et al. (2014). Seasonal and spatial methane dynamics in the water column of the central Baltic Sea (Gotland Sea). *Continental Shelf Research*, *91*, 12–25. https://doi.org/10.1016/j.csr.2014.07.005

Niemann, H., Steinle, L., Blees, J., Bussmann, I., Treude, T., Krause, S., et al. (2015). Toxic effects of lab-grade butyl rubber stoppers on aerobic methane oxidation. *Limnology and Oceanography: Methods*, *13*(1), 40–52. https://doi.org/10.1002/lom3.10005

Pawlowicz, R., Beardsley, B., & Lentz, S. (2002). Classical tidal harmonic analysis including error estimates in MATLAB using T_TIDE. *Computers & Geosciences*, *28*(8), 929–937. https://doi.org/10.1016/S0098-3004(02)00013-4

Pernthaler, A., Pernthaler, J., & Amann, R. (2002). Fluorescence in situ hybridization and catalyzed reporter deposition for the identification of marine bacteria. *Applied and Environmental Microbiology*, *68*(6), 3094–3101. https://doi.org/10.1128/AEM.68.6.3094-3101.2002

Schmale, O., Walter, M., Schneider von Deimling, J., Sültenfuß, J., Walker, S., Rehder, G., & Keir, R. (2012). Fluid and gas fluxes from the Logatchev hydrothermal vent area. *Geochemistry, Geophysics, Geosystems*, *13*(7), Q07007. https://doi.org/10.1029/2012GC004158

Schneider von Deimling, J. (2017). Cruise Report R/V POSEIDON POS504 - Seepage process analyses at the abandoned well Blowout site (22/4b, North Sea), 27.08.2016 – 09.09.2016 (Kiel - Kiel) (p. 44). Kiel: Christian-Albrechts-Universität zu Kiel. https://doi.org/10.3289/CR_POS504

Wilson, S. T., Bange, H. W., Arévalo-Martínez, D. L., Barnes, J., Borges, A. V., Brown, I., et al. (2018). An intercomparison of oceanic methane and nitrous oxide measurements. *Biogeosciences*, *15*(19), 5891–5907. https://doi.org/10.5194/bg-15-5891-2018